

Unifying Distillation with Personalization in Federated Learning

Siddharth Divi
Purdue University
West Lafayette, USA
sdivi@purdue.edu

Habiba Farrukh
Purdue University
West Lafayette, USA
hfarrukh@purdue.edu

Z Berkay Celik
Purdue University
West Lafayette, USA
zcelik@purdue.edu

ABSTRACT

Federated learning (FL) is a decentralized privacy-preserving learning technique in which clients learn a joint collaborative model through a central aggregator without sharing their data. In this setting, all clients learn a single common predictor (FedAvg), which does not generalize well on each client’s local data due to the statistical data heterogeneity among clients. In this paper, we address this problem with PERSFL, a discrete two-stage personalized learning algorithm. In the first stage, PERSFL finds the optimal teacher model of each client during the FL training phase. In the second stage, PERSFL distills the useful knowledge from optimal teachers into each user’s local model. The teacher model provides each client with some rich, high-level representation that a client can easily adapt to its local model, which overcomes the statistical heterogeneity present at different clients. We evaluate PERSFL on CIFAR-10 and MNIST datasets using three data-splitting strategies to control the diversity between clients’ data distributions. We empirically show that PERSFL outperforms FedAvg and three state-of-the-art personalization methods, pFedMe, Per-FedAvg and FedPer on majority data-splits with minimal communication cost. Further, we study the performance of PERSFL on different distillation objectives, how this performance is affected by the equitable notion of fairness among clients, and the number of required communication rounds. PERSFL code is available at <https://tinyurl.com/hdh5zhxs> for public use and validation.

1 INTRODUCTION

Federated Learning (FL) is a distributed collaborative learning paradigm that does not require centralized data storage in a single location. Instead, a joint global predictor is learned jointly by a network of participating users [20]. This paradigm is useful when the clients have private data that they cannot share with the participating entities due to privacy concerns. Recently, FL has found widespread applications in domains ranging from healthcare, finance to predictive keyboards.

Federated Averaging (FedAvg) [20] is an algorithm in which n users along with a central global aggregator participate together to learn a joint collaborative model. The data of each user does not leave their device. The users train the shared model on their local data and then share their model weights to the central aggregator. The central aggregator then aggregates (averages) the model updates from all the participating users and shares the new global shared model’s updated weights. This process continues till convergence. In the end, each user obtains the same global model.

Statistical Data Heterogeneity Problem. FL faces different challenges such as expensive communication, systems heterogeneity, statistical heterogeneity, and privacy concerns [15]. Among these, statistical data heterogeneity has recently gained attraction, which

means that clients’ data are unbalanced and non-identical and independently distributed (non-IID). Thus, the global model trained on clients’ non-IID data restricts the global FL model from delivering good generalization on each client’s local data. Each client gets a common model, irrespective of their data distribution. For instance, consider the next word prediction engine that outputs what word comes next suggestions on a smartphone that enables users to express themselves faster. A common model learned collaboratively among clients fails to give each user useful suggestions, particularly when they have a unique way of expressing themselves in mobile applications such as in writing texts or emails. On the other hand, learning without client collaboration leads to a poor generalization of local clients due to a lack of data. Personalized learning schemes proposed for FL aim to address this problem by finding a personalized model for each client that benefits from other clients’ data while overcoming the statistical heterogeneity problem.

Personalization Approaches. There have been a few different approaches that proposed learning schemes through meta-learning, local fine-tuning, multi-task learning, model regularization, contextualization, and model interpolation to build personalized models. For instance, Per-FedAvg uses Meta-Learning [6, 12] to learn a common initialization point for all the users, which is then adapted to each user with a couple of steps of gradient descent. Another approach, pFedMe [5], re-formulates the FL objective as a bi-level optimization problem and modifies the minimized loss function with the inclusion of a regularization term. Lastly, FedPer [1] splits a deep neural network into base and personalization layers, where the base layers are learned collaboratively, and personalization layers are specific to each user. However, some of these approaches incur high computational and algorithmic complexity. For instance, pFedMe and Per-FedAvg require a higher number of global communication rounds compared to FedPer. Model Agnostic Meta-Learning based methods (MAML) [7] (used in Per-FedAvg) require the computation of the Hessian matrix, which significantly adds computational complexity to each client.

Contributions. In this paper, we introduce PERSFL, a new discrete two-stage personalization algorithm, which distills each client’s optimal teacher model into each client’s local model. In the first stage, each client participates in the FL training and stores the global model from the aggregator at each communication iteration. At the end of the FL training, clients measure each global model’s validation error and set the model that gives the least error as an optimal teacher. Teacher models contain useful information unique to each client that can be readily adapted into the local models. At the end of the first stage, each client obtains a separate teacher model and proceeds to the second stage. In the second stage, each client distills the information from the optimal teacher model into their local model to learn a personalized model. PERSFL

controls the trade-off between optimal teacher and local model with temperature parameter that scales the class probability predictions from the teacher, and imitation parameter that balances how much a client imitates the teacher. At the end of PERSFL algorithm, each client trains a local model based on their dataset and the useful knowledge extracted from other clients’ datasets.

We empirically demonstrate the effectiveness of PERSFL using CIFAR-10 and MNIST datasets, which are widely used to evaluate personalized models’ performance. We compare PERSFL with FedAvg and three recent approaches of personalization in FL, a transfer-learning based algorithm (FedPer), a bi-level optimization based algorithm (pFedMe), and a meta-learning based algorithm (Per-FedAvg). To have a fair comparison, we use three different data-splitting strategies to control how each client’s local dataset differs from other clients’ data.

Our extensive experiments demonstrate that PERSFL outperforms FedAvg, and outperforms or yields comparable results with the FedPer, pFedMe and Per-FedAvg in local accuracy. For example, compared to the best performing methods on CIFAR-10 data-splits, PERSFL improves the accuracy of users on average by 4.7%, 0.6% and 3.9% over FedPer, pFedMe, and FedPer, respectively. We perform additional experiments to characterize the equitable notion of fairness—the deviation among per-user accuracy, study the performance of variants of distillation objectives and investigate the number of communication rounds for convergence. For instance, PERSFL reduces the deviation of per-user accuracy distributions on average by 1.5x and 1.67x compared to Per-FedAvg and FedPer algorithms on two different data-splits on MNIST. For the number of global communication rounds, PERSFL takes 0.03x and 0.5x less communication rounds than pFedMe and FedPer on two different data-splits on CIFAR-10. We show that these results challenge the existing objectives of personalized learning schemes and motivate new problems in personalization for the research community.

2 RELATED WORK

Several prior works have explored techniques for personalization in FL instead of using a common model for all users. These works can be broadly grouped into the following categories based on the techniques adapted to improve clients’ model performance, such as personalization via meta-learning, local fine-tuning, multi-task learning, model regularization, contextualization, and model interpolation. Below, we review the recent core approaches.

Per-FedAvg [6] uses MAML to learn an initialization point for each user, adapted to their local data after the training phase. In a closely related work, Personalized FedAvg [13], a variant of Federated Averaging through Reptile algorithm, interprets FedAvg as a linear combination of a naive baseline and existing MAML methods.

pFedMe [5] formulates a bi-level optimization problem using the Moreau envelope as users’ regularized loss function, thereby separating personalized model optimization from the global model learning. MOCHA [21] extends multi-task learning to the FL setting to overcome the ill-effects of statistical heterogeneity. Though this scheme leads to more user-specific solutions, it requires all the participating users to be available at all times during training.

Adaptive Personalized Federated Learning (APFL) [4] learns a personalized model for each user that is a mixture of the local and

global models. The optimal mixing parameter, which controls the local and global models’ ratio, is integrated into the learning problem. Another approach FedPer [1] divides a deep neural network into the base and personalization layers to learn the base layers collaboratively and personalization layers specific to each user.

In a recent work [19], three different approaches have been proposed with generalization guarantees, user clustering, data interpolation, and model interpolation. The first two approaches are not suitable for FL since they require meta-feature information from the clients, which raises privacy concerns. The third approach interpolates the local and global models and is closely related to the formulation of APFL method.

Another work, LotteryFL [14] adopts a Lottery Ticket Network through Lottery Ticket Hypothesis [8] to learn personalized models for each user. Lastly, FedBE [3] integrates Bayesian learning into models to perform an aggregation of client uploaded model weights where the central aggregator creates a Bayesian model ensemble based on the client models.

In contrast to the previous works, we use a modified formulation of the federated learning problem that incorporates distillation with each user’s unique optimal teacher to train a per-user model based on their local dataset and other users’ datasets.

3 PRELIMINARIES

Model compression [2] or distillation [10] are techniques to reduce the size and complexity of machine learning models. Distillation compresses a large complex model or an ensemble of models $f_{\text{large}}(x)$ (teacher model) into a smaller and less complex model $f_{\text{small}}(x)$ (student model), which mimics the predictions of the complex model. There are scenarios in which the teacher model and ensemble models are too complicated from a computational perspective. Thus, distilling a large model into a simpler model makes it easier to run on limited computational resources such as on edge and mobile devices. Remarkably, model distillation achieves model compression with no or minimal loss in accuracy.

Put in math, given a large model f_{large} that has been already learned, a small model f_{small} is learned by minimizing

$$f_s = \arg \min_{f_{\text{small}} \in F_s} \frac{1}{n} \sum_{i=1}^n [(1 - \lambda) \mathcal{L}(\{(x_i, y_i)\}_{i=1}^n, f_{\text{small}}) + \lambda \mathcal{L}(\{(x_i, s_i)\}_{i=1}^n, f_{\text{small}})] \quad (1)$$

where f_{small} is the candidate student model from the class capacity measure of the student model F_s (i.e., hypothesis space of models for the student model), f_s is the optimal student model learned, and $\lambda \in [0, 1]$ is the imitation parameter which controls how much f_{small} imitates f_{large} compared to directly learning from the data.

In Equation 1, there are two datasets on which f_{small} is trained, $(x_i, y_i)_{i=1}^n$ and $(x_i, s_i)_{i=1}^n$. s_i is called the soft label of the f_{large} model computed as $s_i = f_{\text{large}}(x_i)/T$ and y_i is the ground truth label. $T > 0$ is called the temperature parameter, which softens the teacher model’s class probabilities. The softened class-probability predictions reveal dependencies among the labels that are otherwise hidden as either being extremely small or large numbers.

Algorithm 1 PERSFL Algorithm

```
1: Stage-1: Finding the optimal teacher models
2: Notation:
   K: Clients indexed by k,  $E_G$ : Number of global aggregation rounds,  $\mathcal{G}_e$ : Global FedAvg model during the global aggregation round e,  $O_k$ :
   Optimal teacher model for user k,  $l_k$ : Loss of  $O_k$  on the user k's validation data (initialized to an arbitrarily large value),  $x_k^{val}$ : Validation
   data of user k.
3: for global aggregation round e = 1 to  $E_G$  do
4:   for user k = 1 to K do
5:      $l_k \leftarrow \mathcal{L}_{cross}(\sigma(\mathcal{G}_e(x_k^{val})), y_k^{val})$ 
6:     if  $l_k < l_{k'}$  then
7:        $l_{k'} \leftarrow l_k$ 
8:        $O_k \leftarrow \mathcal{G}_e$ 
9:     end if
10:  end for
11: end for


---


12: Stage-2: Distilling from the optimal teacher models
13: Notation:
   K: Clients indexed by k, B: Local mini-batch size,  $E_L$ : Number of local epochs, T: Temperature parameter,  $\lambda$ : Imitation parameter,  $O_k$ :
   Optimal teacher model for user k,  $A_k$ : Local personalized model of user k,  $|T|_c$ : Search space of temperature values,  $|\lambda|_c$ : Search space of
   imitation parameter values.
Client Side:

- For each client k, initialize  $A_k$  with the weights of  $O_k$ .
- Find the optimal values of  $\lambda$  and T by performing the following steps.


14: for user k = 1 to K do
15:   B  $\leftarrow$  Obtain user k's training data
16:   for local epoch i = 1 to  $E_L$  do
17:     for batch b  $\in$  B do
18:        $\mathcal{L}(A_k, b) \leftarrow (1 - \lambda) * \text{hardLoss} + (\lambda T^2) * \text{softLoss}$ 
19:        $\text{hardLoss} \leftarrow \mathcal{L}_{cross}(y_b, \sigma(A_k(b)))$ 
20:        $\text{softLoss} \leftarrow \mathcal{KL}(s_b, \sigma(\frac{A_k(b)}{T}))$ 
21:        $s_b \leftarrow \sigma(\frac{O_k(b)}{T})$ 
22:        $w \leftarrow w - \eta \nabla \mathcal{L}(A_k, b)$ 
23:     end for
24:   end for
25: end for
```

4 UNIFYING DISTILLATION WITH PERSONALIZATION

We introduce PERSFL, a new personalization algorithm, which unifies distillation with personalization to improve the generalization of each user's model accuracy instead of using the same global FedAvg model for each user.

4.1 PERSFL Algorithm

Our idea of distillation for personalization is inspired by the discrete phase local adaptation technique called the greedy local fine-tuning method [4]. In this approach, a global FedAvg model is first learned during the training phase. During the subsequent adaptation phase, users perform several gradient descent steps to adapt the global FedAvg model's weights to users' local data distribution. However, a crucial question that needs to be answered is: *why do all users adapt the same global model when the goal is personalization for each user?* This question inspires us to integrate a separate optimal teacher

model into the local model of each user. To obtain the optimal teacher, each user iteratively validates the global FedAvg model on their local data during each aggregation round of the FL training phase. Subsequently, each user identifies the best global FedAvg model as an optimal teacher based on the accuracy. Each user then incorporates the optimal teacher into their local model through distillation. Algorithm 1 details the steps of the PERSFL, which is a discrete two-stage algorithm.

Stage-1: Finding the optimal teacher models. In the first stage, each user participates in the training phase of FL and receives the current copy of the global model (FedAvg) in each round. In this step, each user locally stores the global model's current copy before updating the local version of the global model and sending it to the server for aggregation. After the termination of the FL training phase, each user finds the optimal teacher model O_k by minimizing:

$$O_k = \arg \min_{O_{k'} \in |G|_E} \mathcal{L}_{cross}(\sigma(O_{k'}(x_k^{val})), y_k^{val}) \quad (2)$$

where $|G|_E$ is the FedAvg model learned in each global aggregation round, E is the total number of global aggregation rounds of FL, x_k^{val} is the validation data of user k and y_k^{val} is the ground truth of the validation data of user k . Thus, the optimal teacher model represents the global FedAvg model across the aggregation rounds that achieves the minimum loss on the validation data of user k .

Stage-2: Distilling from the optimal teacher models. The second stage takes place locally for each user after the FL training phase, independent of FL (i.e., no client collaboration). We call this stage local adaptation. We first initialize the personalized model, A_k with the weights of O_k for each user k . Following this, each user distills the information from the optimal teacher (O_k) into their local model to learn A_k . Specifically, each user computes A_k by distilling hard-loss and soft-loss by minimizing:

$$A_k = \arg \min_{\substack{\lambda' \in |\lambda|_C, T' \in |T|_C \\ A_{k'} \in |A_k|_C}} \underbrace{(1 - \lambda') (\mathcal{L}_{\text{cross}}(\sigma(A_{k'}(x_k^{\text{train}})), y_k^{\text{train}}))}_{\text{hard-loss}} + \underbrace{(\lambda' T'^2) \times \mathcal{KL}(\sigma(\frac{A_{k'}(x_k^{\text{train}})}{T'}), \sigma(\frac{O_{k'}(x_k^{\text{train}})}{T'}))}_{\text{soft-loss}} \quad (3)$$

The hard-loss refers to the loss of the student model (A_k) on the hard-labels (y_i), whereas soft-loss refers to the loss of the student model on the soft labels (s_i). Soft labels are the teacher model's (O_k) scaled predictions. $|\lambda|_C$ refers to the complexity of the search space of the imitation parameter, $|T|_C$ denotes the search space complexity of the temperature parameter, and $|A_k|_C$ refers to the hypothesis space of the personalized models for k . Here, each user performs a grid-based search to find the optimal values for distillation parameters temperature (T) and imitation parameter (λ) while simultaneously learning the personalized model.

We use Kullback-Leibler (KL) divergence between the output of the teacher model (O_k) and the student model (A_k). Enforcing the logits of O_k and A_k to be similar yields a regularizing effect, which in turn improves the generalization ability of A_k . We additionally multiply the soft-loss by T^2 since the gradients of the term $\sigma(A_k(b)/T)$ scale as $1/T^2$. This ensures that the relative contributions of the hard-labels (y_i) and the soft-labels (s_i) are roughly unchanged if the T value changes.

At the end of the **Stage-2**, each user learns a personalized model optimized for their local data distribution by distilling the useful knowledge from other users into the personalized model A_k through the optimal teacher O_k learned in **Stage-1**.

4.2 Why Does PERSFL Work?

We introduce the learning under privileged information (LUPI) paradigm [22] and show that PERSFL reduces to Generalized Distillation [18], an instance of the LUPI paradigm. Vapnik's LUPI paradigm assumes that feature-label pairs (x_i, y_i) , and additional information x_i^* about (x_i, y_i) are available at training time and x_i^* is not available at test time. Here, x_i^* is called the privileged information. For example, consider the problem of identifying cancerous biopsy images. x is the biopsy image of a patient in pixel

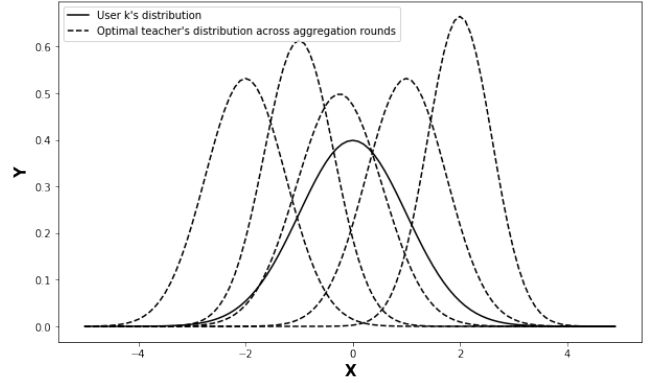


Figure 1: Users k 's distribution vs. global FedAvg model's distribution across the global aggregation rounds.

space. An oncologist may describe the biopsy image relevant to cancer in a specialized language space different than the pixel space. The descriptions are called privileged information (x^*), which contain useful information to classify the biopsy images, however this information is not available at test time.

Generalized distillation develops an objective to learn from multiple data representations as follows. First, it learns a teacher model f_t on the feature-target set $\{x_i^*, y_i\}_{i=1}^n$. Second, it computes teacher soft labels $s_i = f_t(x_i^*)/T$ using a temperature parameter $T > 0$. Lastly, it learns a student model f_s from $\{x_i, y_i\}_{i=1}^n, \{x_i, s_i\}_{i=1}^n$.

In PERSFL, the optimal teacher model O_k of each user k is analogous to the privileged information x^* . Since each user's data distributions are not exactly the same, each user's optimal teacher model is unique and identified with the best performing FedAvg model on the user i 's validation data during the FL communication rounds. A user can obtain the intricate patterns from other users' large amounts of data through the weights of O_k as privileged information, only available to each user during FL training.

Once each user identifies the teacher model, the soft-labels of the teacher model (s_i) are computed on the data of each user. PERSFL learns the student model from the teacher through distillation by choosing optimal values of the parameters, λ and T . We argue that distilling information from the teacher model to the student model overcomes the *catastrophic forgetting* problem [9], which is the tendency of a model to forget the information learned in the previously trained tasks when it is trained on new tasks. PERSFL mitigates this problem by first initializing the student model with the teacher model's weights and then distilling the teacher model's information to the student model.

Figure 1 shows the training data distribution of a user k (solid line) and the distribution of the FedAvg model in the global communication rounds (dashed lines). The global model's distribution comes close to approximating the user's distribution and starts moving away from it. This divergence of distributions is caused due to the non-IID data distribution across users. PERSFL's teacher model is unique to each user, and there is maximal overlap with their data distribution, which helps address the statistical heterogeneity

problem and mitigate its negative transfer effect. Our extensive experiments in Section 5 validate this hypothesis.

4.3 Convergence and Complexity Analysis

Convergence of PERSFL. Convergence of an algorithm is defined as the algorithm’s ability to converge to the global optimum, which is defined as the region in the loss landscape with the lowest possible loss (global minima). Equation 4 represents the core objective of the FL setting. Here, $f_i(\cdot)$ denotes the expected loss over the data distribution of user i when there are N users, and w refers to the weights of the FedAvg model being learned.

$$\min_{w \in \mathcal{R}^d} \left\{ f(w) := \frac{1}{N} \sum_{i=1}^N f_i(w) \right\} \quad (4)$$

Unlike other personalized FL methods such as pFedMe and FedPer, the convergence analysis for PERSFL is not needed since PERSFL does not modify the FL core objective. To detail, PERSFL is a two-stage discrete algorithm in which the users join the FL training in the first stage to learn a separate optimal teacher model. Each user then independently distills the optimal teacher to their local dataset. Therefore, the convergence of PERSFL is the same as the convergence of the FedAvg algorithm [17].

Complexity of PERSFL. We analyze the complexity of PERSFL in terms of the number of epochs executed locally at each user during the training phase. The worst-case complexity of PERSFL when all users are computationally involved in every round is given by $\mathcal{O}(E_G E_L + |T|_C |\lambda|_C E)$. E_G is the number of global communication rounds, E_L is the number of local epochs, $|T|_C$ and $|\lambda|_C$ are the class complexity measures of the search space and E is the number of epochs that we set to distill information from the optimal teacher model into the personalized model.

5 EXPERIMENTS

We evaluate the performance of PERSFL using two datasets, each with three data-splits, and compare its results with FedAvg and three recent personalization approaches, FedPer, pFedMe, and Per-FedAvg. Table 1 describes the compared approaches with PERSFL, including the datasets used in their evaluation, data-splits (detailed below), and the algorithms that they compare with their techniques.

We conduct all the experiments with 10 users. We make three assumptions in line with the assumptions made in compared approaches. First, we assume that all users are active during the entire training phase to speed up the model convergence. Second, the data of each user does not change between the global aggregations. Lastly, the hyper-parameters, batch-size (B), and local epochs (E), are invariant among the participant users. We conduct all experiments with a 60%-20%-20% train-validation-test split on an NVIDIA Tesla T4 GPU with 16GB memory.

Datasets and Datasplits. We evaluate PERSFL on the CIFAR-10 and MNIST datasets. These datasets are widely used in FL training and are also used by the compared methods. To have a fair comparison, we use three different data-splits for both the CIFAR-10 and MNIST. MNIST is a dataset of 28×28 images of handwritten digits from 0-9 consisting of 10 labels and 70,000 instances. CIFAR-10 is a dataset of 32×32 color images with 10 classes and 60,000 instances.

#	Method	Datasets	Comparison	Datasplit
1	Per-FedAvg [6]	MNIST, CIFAR10	FedAvg	Custom
2	pFedMe [5]	MNIST, Synthetic dataset	FedAvg, Per-FedAvg	DS-3
3	FedPer [1]	FLICKR-AES, CIFAR-10, CIFAR-100	FedAvg	DS-1

Table 1: The details of the personalized federated learning methods compared with PERSFL.

In data-split 1 (**DS-1**), each user has the same total number of samples but may have different classes and a different number of samples per class. The statistical heterogeneity is varied by controlling the parameter k , which controls the number of overlapping classes between each user. For example, $k = 4$ corresponds to a highly non-identical data partition, whereas $k = 10$ corresponds to a highly identical data partition across the participating users. In our experiments, we set k to 4 to have non-IID data across users.

In **DS-2**, all users have samples from all classes, but the number of samples per class they have is different, and hence the total number of samples per user is also different across users. In order to simulate a non-IID distribution, we assign samples from each class to the users using a Dirichlet distribution with $\alpha = 0.9$, following the previous work [11]. Each class is parameterized by a vector q where $q \geq 0$, $i \in [1, N]$, where q is sampled from a Dirichlet distribution with parameters α and p . The parameter p is the prior class distribution over the classes, and α is the concentration parameter that controls the data similarity among the users. If $\alpha \rightarrow \infty$, all users have an identical distribution to the prior. If $\alpha \rightarrow 0$, each user only has samples from one class randomly chosen.

For **DS-3**, each user has two of the ten class-labels. Additionally, the total number of samples per user is different, i.e., all the users do not have the same number of total samples. The samples assigned to users are drawn from a log-normal distribution with the parameters $\mu = 0$ and $\sigma = 2$. A variable u has a log-normal distribution if $\log(u)$ is normally distributed. The probability density function for the log-normal distribution is computed as:

$$p(u) = \frac{1}{\sigma u \sqrt{2\pi}} e^{-\left(\frac{\ln(u)-\mu}{\sigma}\right)^2} \quad (5)$$

These parameters correspond to the underlying normal distribution from which we draw the samples.

Model Architecture. For the CIFAR-10 dataset, we use a CNN-based model with two 2-D convolutional layers separated by a MaxPool layer between them and followed by three fully connected (FC) layers. The fully connected layers have 400, 120, and 84 hidden neurons. We use ReLU activations after each layer except the last FC layer. For the MNIST dataset, we use a two-layer deep neural network (DNN) with 100 hidden-layer neurons. We use a ReLU activation on the hidden layer. The output layer has 10 nodes with a softmax function to get the class probabilities. The architectures we use for both datasets are similar to those in pFedMe for conformity.

5.1 Degree of Personalization across Users

To study the degree (extent) of personalization of PERSFL and to compare it with the other personalization approaches, we average experiments of CIFAR-10 and MNIST datasets over 5 experimental runs for each data-split. Table 2 and Table 3 show the per-user

Users	FedAvg			PERSFL			FedPer			pFedMe			Per-FedAvg		
	DS-1	DS-2	DS-3	DS-1	DS-2	DS-3	DS-1	DS-2	DS-3	DS-1	DS-2	DS-3	DS-1	DS-2	DS-3
User 0	43.6	50.8	48.2	85.5	61.3	94.5	83.2	57.2	93.1	74.3	61.7	94.2	69.2	58.2	92.5
User 1	50.9	45.3	40.8	78.2	56.9	79.9	74.5	51.4	77	64.1	57.3	79.2	65	56.1	73.7
User 2	44.5	49.4	31.2	82.2	57.3	68.9	78.4	53.2	64.7	69.6	57.3	64.4	67.9	57.2	64.6
User 3	51.3	46.5	31.5	82.1	60.1	82.5	77.9	55.4	77.5	69.4	58.9	72.5	67.2	58.8	77
User 4	45.3	50.8	49.4	79.4	59.1	82.5	76.1	54.4	78.6	67.2	59.5	80	65.8	59.4	82.5
User 5	44.2	50.7	47.8	77.1	61.9	79.9	72.1	57.6	76.9	62.1	60.6	77.5	62.7	59.3	77.9
User 6	35.8	46.5	56.8	75.6	58.9	90.3	70.9	53.3	88.5	59.9	58.6	88.3	58.2	57.7	89.1
User 7	37.9	49.5	58.1	79.7	61.2	87.6	75.6	56.9	84.6	65.8	60.2	84	64.3	58	83.7
User 8	47.7	48.7	49	87.7	60	76.7	84.4	57.5	73.5	75.5	59.6	66.9	72.5	55.8	64.1
User 9	48.6	49.1	53.5	91	58.8	80.3	88.5	54.3	77.9	81.7	58.3	73.8	76.6	55.3	72.7
Avg. Acc.	45	48.7	46.6	81.9	59.6	82.3	78.2	55.1	79.2	69	59.2	78.1	66.9	57.6	77.8
Std Dev	5.1	2	9.4	4.9	1.7	7.2	5.6	2.1	7.9	6.7	1.4	9.2	5.1	1.5	9.5

Table 2: Accuracy per user for the different personalization algorithms on the different data-splits on the CIFAR-10 dataset.

Users	FedAvg			PERSFL			FedPer			pFedMe			Per-FedAvg		
	DS-1	DS-2	DS-3	DS-1	DS-2	DS-3	DS-1	DS-2	DS-3	DS-1	DS-2	DS-3	DS-1	DS-2	DS-3
User 0	91.2	84.2	98.3	98.3	88.6	99.6	98.2	84.2	99.9	94.8	88.2	99	97.3	87.5	98.6
User 1	92.2	85.2	97.9	98.8	86.3	99.3	98.8	85.2	99.3	95.8	86.1	98.3	99	86.1	97.6
User 2	88	83.5	96.2	99.5	86	98.7	98.3	83.5	98.2	93.2	85.4	97.5	99.7	86.2	96.8
User 3	93.2	84.4	94.8	98.2	87.9	99.6	97.8	84.4	99.6	94.3	86.7	97.6	98.7	87.5	96
User 4	92.3	86.6	96.3	98.7	88.1	99.6	98.2	86.6	99.6	93.7	87.4	98.1	99	88	97.1
User 5	92.2	84.5	97.3	98.3	86.4	99.2	97.8	84.5	99.1	94.2	85.3	98.5	98.8	86.8	97.7
User 6	93.8	87	97.7	98.7	88.8	99.8	98.5	87	99.9	95	88	98.8	99.2	87.9	98.2
User 7	91.5	86.8	95.7	98.7	88.7	99.6	98.5	86.8	99.4	95.8	87.7	98	99.3	88.2	96.9
User 8	94.3	85.8	94.3	98.3	89.1	99.2	98.3	85.8	98.9	94.5	87.9	97.8	98.8	88.5	96.5
User 9	91.3	86.7	95.9	98.5	89.7	99.7	98.5	86.7	99.6	96.2	88.6	98.3	99.2	89.1	97.4
Avg Acc	92	85.5	96.4	98.6	88	99.4	98.3	85.5	99.4	94.8	87.1	98.2	98.9	87.6	97.3
Std Dev	1.7	1.3	1.3	0.4	1.3	0.3	0.3	1.3	0.5	1	1.2	0.5	0.6	1	0.8

Table 3: Accuracy per user for the different personalization algorithms on the different data-splits on the MNIST dataset.

accuracy of Fed-Avg, PERSFL, FedPer, pFedMe, and Per-FedAvg on different datasplits of CIFAR-10 and MNIST. Below, we present the performance of PERSFL with the FedAvg model and the best performing algorithm on the average accuracy across users.

Our analysis of CIFAR-10 in Table 2 shows that PERSFL performs better than other personalization techniques across all data-splits. In comparison to the FedAvg model, PERSFL leads to a percentage increase of 82%, 22.3%, and 76.6% on **DS-1**, **DS-2**, and **DS-3**. For the compared approaches, for all data splits, PERSFL improves the on average accuracy by 4.7%, 0.6% and 3.9% across users compared to FedPer, pFedMe, and FedPer respectively. The absolute improvement of PERSFL over other techniques on **DS-1**, **DS-2** and **DS-3** is 3.7%, 0.4% and 3.1%, compared to FedPer, pFedMe, and FedPer.

The results of our experiments on MNIST in Table 3 show that, in comparison to the FedAvg model, PERSFL improves the accuracy on average by 7.1%, 2.9%, and 3.1% on **DS-1**, **DS-2**, and **DS-3**. PERSFL performs similar to the other approaches. In **DS-1**, the best-performing approach Per-FedAvg gives 98.9% accuracy, which performs slightly better than 98.6% accuracy of PERSFL. In **DS-2**, PERSFL gives a 0.4% increase in accuracy across users compared to Per-FedAvg. In **DS-3**, both PERSFL and FedPer gives 99.4% accuracy.

5.2 Equitable Notion of Fairness among Users

To understand the distribution of the personalized models’ performance across users, we compute the standard deviation (SD) of the per-user accuracy. From an equitable notion of fairness, this helps us understand how fair the personalization improvements are across users [16]. For two personalization techniques t and t' , the performance distribution among K users represented by $\{F_1(t), \dots, F_K(t)\}$ is more fair (uniform) under technique t than t' if the following holds:

$$\text{Var}(F_1(t), \dots, F_K(t)) < \text{Var}(F_1(t'), \dots, F_K(t')) \quad (6)$$

We compare PERSFL with the best performing method in terms of average accuracy. In CIFAR-10 experiments (Table 2), PERSFL yields a SD of 4.9 among the average accuracy of users on **DS-1**, which is the least deviation compared to the other approaches. This yields a reduction of 1.14x in SD compared to FedPer. For **DS-2**, pFedMe yields an SD of 1.4, slightly better than 1.7 SD of PERSFL. For **DS-3**, PERSFL achieves a reduction of 1.10x in SD compared to FedPer.

For MNIST (Table 3), we observe similar results compared to the experiments on CIFAR-10. For **DS-1**, although Per-FedAvg with an average 98.9% accuracy is better than PERSFL’s 98.6% accuracy,

Users	DS-1		DS-2		DS-3	
	FedAvg	Opt Teacher	FedAvg	Opt Teacher	FedAvg	Opt Teacher
User 0	84.5	85.5	59.5	61.3	94.6	94.5
User 1	77.6	78.2	55.9	56.9	78.7	79.9
User 2	81.2	82.2	55.7	57.3	68.2	68.9
User 3	81.4	82.1	58.6	60.1	81	82.5
User 4	78.7	79.4	58.1	59.1	82	82.5
User 5	75.2	77.1	60.9	61.9	79.6	79.9
User 6	74.4	75.6	56.6	58.9	90.1	90.3
User 7	79.4	79.7	59.6	61.2	86.9	87.6
User 8	86.6	87.7	58.4	60	75.8	76.7
User 9	90.4	91	56.3	58.8	79.5	80.3
Avg Acc	80.9	81.9	58	59.6	81.6	82.3
Std Dev	5	4.9	1.8	1.7	7.5	7.2

(a) CIFAR-10

Users	DS-1		DS-2		DS-3	
	FedAvg	Opt Teacher	FedAvg	Opt Teacher	FedAvg	Opt Teacher
User 0	98.3	98.3	89	88.6	99.6	99.6
User 1	98.8	98.8	86.3	86.3	99.3	99.3
User 2	99.3	99.5	86.3	86	98.7	98.7
User 3	98.2	98.2	87.9	87.9	99.6	99.6
User 4	98.7	98.7	88.1	88.1	99.6	99.6
User 5	98.3	98.3	86.7	86.4	99.2	99.2
User 6	98.7	98.7	89	88.8	99.8	99.8
User 7	98.7	98.7	89	88.7	99.6	99.6
User 8	98.3	98.3	89	88.1	99.2	99.2
User 9	98.5	98.5	89.6	89.7	99.7	99.7
Avg Acc	98.6	98.6	88.1	88	99.4	99.4
Std Dev	0.3	0.4	1.2	1.3	0.3	0.3

(b) MNIST

Table 4: Average Accuracy across all the users for personalized models initialized with the weights of FedAvg model vs. Optimal Teacher model for each user on (a) CIFAR-10 and (b) MNIST datasets.

PERSFL leads to a 1.5x reduction in SD compared to it. For DS-2, we find that the SD of Per-FedAvg at 1.0, is lower than the SD of PERSFL at 1.3. On DS-3, the reduction factor for PERSFL in SD stands at 1.67x compared to FedPer. Overall, PERSFL often leads to a reduction in the SD of the average accuracy across users, thus leading to a more uniform (fair) distribution than the compared methods.

5.3 Impact of Optimal Teachers on Accuracy

We claim that each user’s optimal teacher model (O_k) has maximal overlap with their local data distribution. To understand the impact of optimal teachers on the degree of personalization of the personalized models, we conduct the following experiment. We compare two different ways of choosing the teacher model, i.e., global FedAvg and optimal teacher models used in Stage-2 of PERSFL as the teacher for distillation. We observe that choosing the optimal teacher model as the teacher and performing distillation leads to more personalized solutions and a lower standard deviation in the per-user accuracy.

Table 4a and Table 4b show the results of using FedAvg and optimal teacher for CIFAR-10 and MNIST datasets. We make the following observations in terms of the average per-user accuracy. On DS-1, initializing with the optimal teacher model leads to a percentage increase of 1.2% and an absolute increase of 1%. On DS-2, the optimal teacher initialization leads to a percentage increase of 2.7% and an absolute increase of 1.6%. In the case of DS-3, there is a 0.8% percentage and 0.7% absolute increase attributed to initialization with optimal teachers. Additionally, we observe that PERSFL yields slightly lower standard deviations of per-user accuracy. We conduct the same experiments on the MNIST dataset and present the results in Table 4b. The average accuracy across users and the standard deviations of the average accuracy are very similar across all the methods. We argue that this variation can be attributed to the lack of inter-class variations in the MNIST dataset.

Figure 2 shows the averaged epoch numbers across the different experimental runs for both CIFAR-10 and MNIST, across all data-splits. The users choose their optimal teacher model after participating in the global communication rounds. We observe that the averaged epoch numbers in which the optimal teacher models

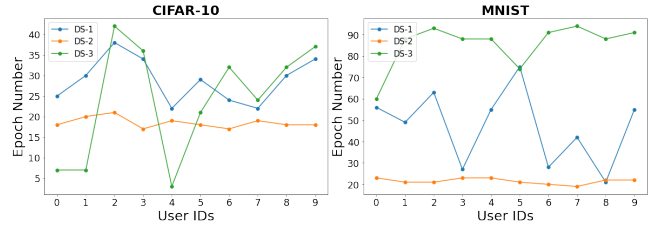


Figure 2: Average epoch numbers when users’ optimal teacher models are selected across data-splits.

Users	CIFAR-10						MNIST					
	DS-1		DS-2		DS-3		DS-1		DS-2		DS-3	
	T	λ	T	λ	T	λ	T	λ	T	λ	T	λ
User 0	12.2	0.45	8.2	0.6	6.6	0.25	1	0	11.4	0.45	1	0
User 1	8.2	0.4	25	0.7	12.2	0.5	1	0	5.8	0.6	1	0
User 2	7.4	0.45	12.2	0.65	2.6	0.3	1.8	0.1	15.4	0.4	1	0
User 3	17	0.3	21	0.6	17	0.35	1	0	10.6	0.45	1	0
User 4	17	0.5	11.4	0.75	11.4	0.15	1	0.05	11.4	0.6	1	0
User 5	12.2	0.55	16.2	0.6	20.2	0.35	1	0.05	1.8	0.65	5.8	0.05
User 6	20.2	0.6	17	0.7	7.4	0.2	1	0.05	11.4	0.4	1	0
User 7	12.2	0.4	2.6	0.65	4.2	0.1	1	0	11.4	0.45	1	0
User 8	12.2	0.5	21	0.75	2.6	0.35	1	0.1	3.4	0.6	1	0
User 9	20.2	0.3	17	0.75	8.2	0.6	1	0	6.6	0.5	1	0

Table 5: Average optimal values of λ and τ for each user across different experimental runs on CIFAR-10 and MNIST.

are chosen are predominantly different. This observation validates our hypothesis that each user has a unique optimal teacher model, and all users should not use the same teacher model. Turning to Figure 1, the dashed curve closest to the solid curve corresponds to the optimal teacher model for a particular user k . The averaged epoch number across all experimental runs at which this optimal teacher model is chosen is shown in Figure 2.

5.4 Optimal Parameter Selection

We conduct experiments to understand distillation’s effectiveness by investigating the values of the optimal distillation parameters chosen by each user’s student model. Table 5 shows the average values of distillation parameters, imitation (λ) and temperature (T), averaged out over the five experimental runs on CIFAR-10 and MNIST datasets. For CIFAR-10, we observe that the λ parameter values are non-zero across users and data-splits. This observation means that distillation is effective, and the teacher model’s knowledge is useful in learning the student model. In contrast, in the case of MNIST, we observe that λ parameter values are mostly very close to 0 in the case of **DS-1** and **DS-3**. We believe that this is because of the nature of the MNIST dataset i.e., due to the lack of inter-class variations. We show a detailed analysis of the variation of the classification accuracy on the test-set across users depending on the values of the distillation parameters λ and T in the Appendix A.

5.5 Variants of PERSFL

The distillation objective of PERSFL in Equation 3 can be implemented with different objective functions defining how to distill the information from the optimal teacher model into the user’s local model. To demonstrate the generalization of PERSFL to different distillation objectives, we perform the distillation with a different loss function and compare it with Equation 3.

We define the following objective function between the soft labels and the student’s soft predictions:

$$A_k = \arg \min_{\substack{\lambda' \in |\lambda|_c, T' \in |T|_c \\ A_{k'} \in |A_k|_c}} \underbrace{(1 - \lambda') (\mathcal{L}_{\text{cross}}(\sigma(A_{k'}(x_k^{\text{train}})), y_k^{\text{train}}))}_{\text{hard-loss}} + \underbrace{(\lambda' T'^2) \times \mathcal{L}_{\text{cross}}(\sigma(\frac{A_{k'}(x_k^{\text{train}})}{T'}), \sigma(\frac{O_{k'}(x_k^{\text{train}})}{T'}))}_{\text{soft-loss}} \quad (7)$$

The soft predictions of a student are defined as the predictions of the student model, which are scaled by the temperature parameter, $\sigma(A_{k'}(x_k^{\text{train}})/T')$. Equation 7 is different from the original formulation of PERSFL in Equation 3. Here we do not use KL-divergence to enforce the similarity of logits between the teacher and student model. In contrast, we compute the cross-entropy between the models. We refer to this variant of PERSFL to PERSFL-GD. We note that other distillation methods can be easily integrated into PERSFL.

Table 6 shows the results of both variants of PERSFL across all data-splits on both CIFAR-10 and MNIST datasets. We make the following three observations. First, in MNIST, both variants of PERSFL on **DS-1** and **DS-3** have a very similar performance in terms of average accuracy across all users. In **DS-2** PERSFL has an absolute performance improvement of 0.7% compared to PERSFL-GD. Second, the performance difference is relatively more in CIFAR-10 experiments. PERSFL has an absolute improvement of 1.4% on **DS-2** of CIFAR-10 and an improvement of 0.6% on **DS-3**. In all cases, PERSFL performs better than or at least equal to PERSFL-GD. Lastly, in terms of the standard deviations between the per-user accuracy, both PERSFL and PERSFL-GD yield very similar performance.

Users	CIFAR-10						MNIST					
	DS-1		DS-2		DS-3		DS-1		DS-2		DS-3	
	①	②	①	②	①	②	①	②	①	②	①	②
User 0	85.5	85.5	61.3	60	94.5	94.1	98.3	98.3	88.6	88.1	99.6	99.8
User 1	78.2	77.8	56.9	56.4	79.9	78.8	98.8	99	86.3	85.3	99.3	99.4
User 2	82.2	81.6	57.3	56.2	68.9	68.2	99.5	99.2	86	85.5	98.7	98.7
User 3	82.1	81.5	60.1	58.4	82.5	82	98.2	98.2	87.9	87.2	99.6	99.8
User 4	79.4	79.2	59.1	58.2	82.5	82.4	98.7	98.5	88.1	87.5	99.6	99.7
User 5	77.1	76.3	61.9	61	79.9	78.8	98.3	98.7	86.4	85.6	99.2	99.3
User 6	75.6	75.5	58.9	57.9	90.3	90.1	98.7	98.5	88.8	88.3	99.8	99.9
User 7	79.7	79.5	61.2	58.8	87.6	87	98.7	99	88.7	88.2	99.6	99.7
User 8	87.7	87.1	60	58.4	76.7	75.6	98.3	98.8	89.1	88.4	99.2	99.3
User 9	91	90.5	58.8	56.3	80.3	79.5	98.5	98.8	89.7	88.7	99.7	99.8
Avg Acc	81.9	81.5	59.6	58.2	82.3	81.7	98.6	98.7	88	87.3	99.4	99.5
Std Dev	4.9	4.9	1.7	1.6	7.2	7.4	0.4	0.3	1.3	1.3	0.3	0.4

Table 6: Performance comparison of variants of PERSFL. ① is for PERSFL, and ② is for PERSFL-GD objective functions.

Method	CIFAR-10			MNIST		
	DS-1	DS-2	DS-3	DS-1	DS-2	DS-3
FedAvg	50	25	100	100	50	100
PERSFL	50	25	50	100	25	100
FedPer	50	25	100	100	50	100
pFedMe	800	1000	800	800	800	800
Per-FedAvg	800	800	1000	800	800	800

Table 7: Comparison of # of global communication rounds

5.6 Global Communication Rounds

In this set of experiments, we compare the number of global communication rounds taken by each personalization algorithm. Table 7 shows the number of global communication rounds for each algorithm. Below, for each dataset’s data-splits, we compare the number of global communication rounds required by PERSFL with the best performing method. We observe that, in CIFAR-10 for **DS-1**, PERSFL takes 50 communication rounds similar to FedPer. For **DS-2**, PERSFL takes 0.03x less communication rounds than pFedMe, and for **DS-3**, PERSFL takes 0.5x less communication rounds than FedPer. In MNIST experiments, we observe that for **DS-1** PERSFL needs 0.13x less communication rounds required by Per-FedAvg. In **DS-2**, PERSFL requires 0.03x less communication rounds compared to Per-FedAvg, and PERSFL needs the same number of communication rounds as FedPer in **DS-3**.

6 DISCUSSION AND LIMITATIONS

Personalization for New Participants. PERSFL can easily adapt new users participating in the FL framework to learn personalized models. To detail, consider that a new user k' joins the framework after the training phase of PERSFL in search of a personalized solution. Since each user chooses their optimal teacher model at the end of the PERSFL training phase, the FedAvg model for user k' may serve as the teacher model i.e., $O_{k'}$ (assuming that only the FedAvg model in the final global aggregation round is stored). If the central aggregator stores the FedAvg model across the global

aggregation rounds, user k' can then choose $O_{k'}$ to be the most optimal FedAvg model across all the global aggregation rounds that has the lowest error on the validation data of user k' . Following this, user k' can then easily perform a search over λ and T to find the optimal values within the search space according to Equation 3. Subsequently, the user can perform distillation with $O_{k'}$ to learn a personalized model $A_{k'}$. However, the global FedAvg model learned over the aggregation rounds may not be the most optimal teacher model for the new participants when the number of new participants joining the framework increases. In future work, we will study the trade-off between the number of new participants and the accuracy of personalized models with respect to the shift in their data distribution.

Dual Optimization of PERSFL. Our work raises some new important questions, such as how to unify distillation with personalization in FL such that personalized models are jointly learned for all users and how to incorporate feedback from the student models to learn more optimal teacher models? Future work will explore the joint learning of the global model and optimal distillation parameters for each user, i.e., joint optimization rather than the discrete formulation of PERSFL. In this way, we plan to incorporate feedback from the student model after distillation to improve each user’s optimal teacher model in the subsequent distillation steps.

An Evaluation Platform for Personalized Models. There exists no common evaluation platform to evaluate the performance of personalized FL models. Our study of various personalized learning schemes shows that the approaches use different datasets and data-splits, and report different evaluation metrics to demonstrate personalized models’ effectiveness. For instance, we observe that per-user accuracy often is not reported, or the equitable notion of fairness is not discussed. In light of these observations, we plan to develop an evaluation framework for personalized FL methods. The evaluation framework will include different real and synthetic datasets and data splitting strategies, and enable future works to easily compare their personalized FL methods with existing approaches in convergence rate, local accuracy, and communication-efficiency.

7 CONCLUSIONS

We present PERSFL¹, a personalized FL algorithm, which addresses the statistical heterogeneity issue between different clients’ data to improve the FL performance. PERSFL finds the optimal teacher model of each client during the FL training phase and distills the useful knowledge from optimal teachers into each user’s local data after the training phase. We evaluate the effectiveness of PERSFL on CIFAR-10 and MNIST datasets using three different data-splitting strategies. Experimentally, we show that PERSFL outperforms the FedAvg and three state-of-the-art personalized FL methods, pFedMe, Per-FedAvg and FedPer on the majority of data-splits with minimal communication cost. We additionally provide a set of numerical experiments to demonstrate the performance of PERSFL on different distillation objectives, how this performance is affected by the equitable notion of fairness among clients, and the number of communication rounds between clients and server.

¹PERSFL code is available at <https://tinyurl.com/hdh5zhxs>.

REFERENCES

- [1] Manoj Ghuhana Arivazhagan, Vinay Aggarwal, Aaditya Kumar Singh, and Sunav Choudhary. 2019. Federated Learning with Personalization Layers. *CoRR* abs/1912.00818 (2019). arXiv:1912.00818 <http://arxiv.org/abs/1912.00818>
- [2] Cristian Bucila, Rich Caruana, and Alexandru Niculescu-Mizil. 2006. Model Compression. In *Proceedings of the 12th ACM SIGKDD International Conference on Knowledge Discovery and Data Mining* (Philadelphia, PA, USA) (KDD '06). Association for Computing Machinery, New York, NY, USA, 535–541. <https://doi.org/10.1145/1150402.1150464>
- [3] Hong-You Chen and Wei-Lun Chao. 2020. FedBE: Making Bayesian Model Ensemble Applicable to Federated Learning. arXiv:2009.01974 [cs.LG]
- [4] Yuyang Deng, Mohammad Mahdi Kamani, and Mehrdad Mahdavi. 2020. Adaptive Personalized Federated Learning. *arXiv e-prints*, Article arXiv:2003.13461 (March 2020), arXiv:2003.13461 pages. arXiv:2003.13461 [cs.LG]
- [5] Canh T. Dinh, Nguyen H. Tran, and Tuan Dung Nguyen. 2020. Personalized Federated Learning with Moreau Envelopes. *arXiv e-prints*, Article arXiv:2006.08848 (June 2020), arXiv:2006.08848 pages. arXiv:2006.08848 [cs.LG]
- [6] Alireza Fallah, Aryan Mokhtari, and Asuman Ozdaglar. 2020. Personalized Federated Learning: A Meta-Learning Approach. *arXiv e-prints*, Article arXiv:2002.07948 (Feb. 2020), arXiv:2002.07948 pages. arXiv:2002.07948 [cs.LG]
- [7] Chelsea Finn, Pieter Abbeel, and Sergey Levine. 2017. Model-Agnostic Meta-Learning for Fast Adaptation of Deep Networks. *arXiv e-prints*, Article arXiv:1703.03400 (March 2017), arXiv:1703.03400 pages. arXiv:1703.03400 [cs.LG]
- [8] Jonathan Frankle and Michael Carbin. 2019. The Lottery Ticket Hypothesis: Finding Sparse, Trainable Neural Networks. In *International Conference on Learning Representations*. <https://openreview.net/forum?id=rjl-b3RcF7>
- [9] Robert M. French. 1999. Catastrophic forgetting in connectionist networks. *Trends in Cognitive Sciences* 3, 4 (1999), 128 – 135. [https://doi.org/10.1016/S1364-6613\(99\)01294-2](https://doi.org/10.1016/S1364-6613(99)01294-2)
- [10] Geoffrey Hinton, Oriol Vinyals, and Jeffrey Dean. 2015. Distilling the Knowledge in a Neural Network. In *NIPS Deep Learning and Representation Learning Workshop*. <http://arxiv.org/abs/1503.02531>
- [11] Tzu-Ming Harry Hsu, Hang Qi, and Matthew Brown. 2019. Measuring the Effects of Non-Identical Data Distribution for Federated Visual Classification. *arXiv e-prints*, Article arXiv:1909.06335 (Sept. 2019), arXiv:1909.06335 pages. arXiv:1909.06335 [cs.LG]
- [12] Yihan Jiang, Jakub Konečný, Keith Rush, and Sreeram Kannan. 2019. Improving Federated Learning Personalization via Model Agnostic Meta Learning. *CoRR* abs/1909.12488 (2019). arXiv:1909.12488 <http://arxiv.org/abs/1909.12488>
- [13] Yihan Jiang, Jakub Konečný, Keith Rush, and Sreeram Kannan. 2019. Improving Federated Learning Personalization via Model Agnostic Meta Learning. arXiv:1909.12488
- [14] Ang Li, Jingwei Sun, Binghui Wang, Lin Duan, Sicheng Li, Yiran Chen, and Hai Li. 2020. LotteryFL: Personalized and Communication-Efficient Federated Learning with Lottery Ticket Hypothesis on Non-IID Datasets. *arXiv e-prints*, Article arXiv:2008.03371 (Aug. 2020), arXiv:2008.03371 pages. arXiv:2008.03371 [cs.LG]
- [15] Tian Li, Anit Kumar Sahu, Ameet Talwalkar, and Virginia Smith. 2020. Federated Learning: Challenges, Methods, and Future Directions. *IEEE Signal Processing Magazine* 37, 3 (May 2020), 50–60. <https://doi.org/10.1109/msp.2020.2975749>
- [16] Tian Li, Maziar Sanjabi, and Virginia Smith. 2019. Fair Resource Allocation in Federated Learning. *CoRR* abs/1905.10497 (2019). arXiv:1905.10497 <http://arxiv.org/abs/1905.10497>
- [17] Xiang Li, Kai xuan Huang, Wenhao Yang, Shusen Wang, and Zhihua Zhang. 2020. On the Convergence of FedAvg on Non-IID Data. *ArXiv* abs/1907.02189 (2020).
- [18] David Lopez-Paz, Léon Bottou, Bernhard Schölkopf, and Vladimir Vapnik. 2016. Unifying distillation and privileged information. In *4th International Conference on Learning Representations, ICLR 2016, San Juan, Puerto Rico, May 2-4, 2016, Conference Track Proceedings*, Yoshua Bengio and Yann LeCun (Eds.). <http://arxiv.org/abs/1511.03643>
- [19] Yishay Mansour, Mehryar Mohri, Jae Ro, and Ananda Theertha Suresh. 2020. Three Approaches for Personalization with Applications to Federated Learning. *arXiv e-prints*, Article arXiv:2002.10619 (Feb. 2020), arXiv:2002.10619 pages. arXiv:2002.10619 [cs.LG]
- [20] H. Brendan McMahan, Eider Moore, Daniel Ramage, and Blaise Agüera y Arcas. 2016. Federated Learning of Deep Networks using Model Averaging. *CoRR* abs/1602.05629 (2016). arXiv:1602.05629 <http://arxiv.org/abs/1602.05629>
- [21] Virginia Smith, Chao-Kai Chiang, Maziar Sanjabi, and Ameet S Talwalkar. 2017. Federated Multi-Task Learning. In *Advances in Neural Information Processing Systems*, I. Guyon, U. V. Luxburg, S. Bengio, H. Wallach, R. Fergus, S. Vishwanathan, and R. Garnett (Eds.), Vol. 30. Curran Associates, Inc., 4424–4434. <https://proceedings.neurips.cc/paper/2017/file/6211080fa89981f66b1a0c9d55c61d0f-Paper.pdf>
- [22] Vladimir Vapnik and Akshay Vashist. 2009. A new learning paradigm: Learning using privileged information. *Neural Networks* 22, 5-6 (2009), 544–557. <http://dblp.uni-trier.de/db/journals/nn/nn22.html#VapnikV09>

A OPTIMAL DISTILLATION PARAMETERS

We present a detailed analysis of the selection of the optimal parameters introduced in 5.4. Figures 3, 4, and 5 show the classification accuracy on the test set of each user for a combination of values of λ and T averaged out over the five experimental runs on CIFAR-10.

Figures 6, 7, and 8 show the classification accuracy in the case of MNIST. The x-axes in these plots represent different values of the imitation parameters, and the y-axes represent the classification accuracy. We do not include the imitation parameter of 1 in these figures because it is never the case in our experiments that the optimal value of λ turns out to be 1.

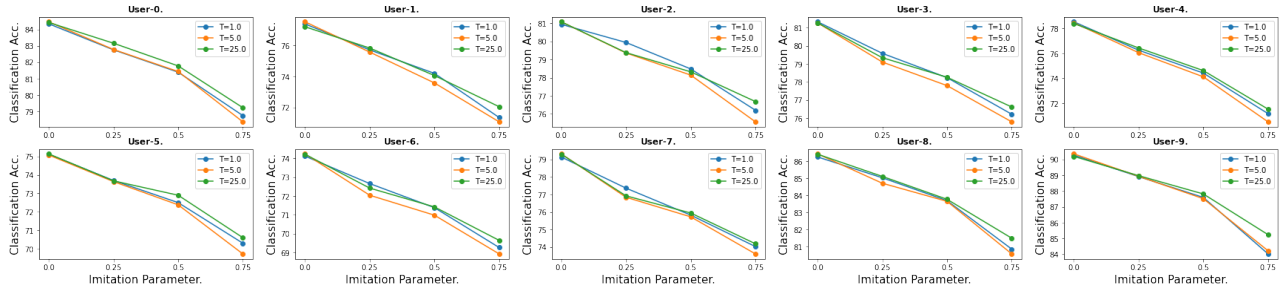


Figure 3: Per-user interaction plots between λ and T on DS-1 of CIFAR-10 averaged over the experimental runs.

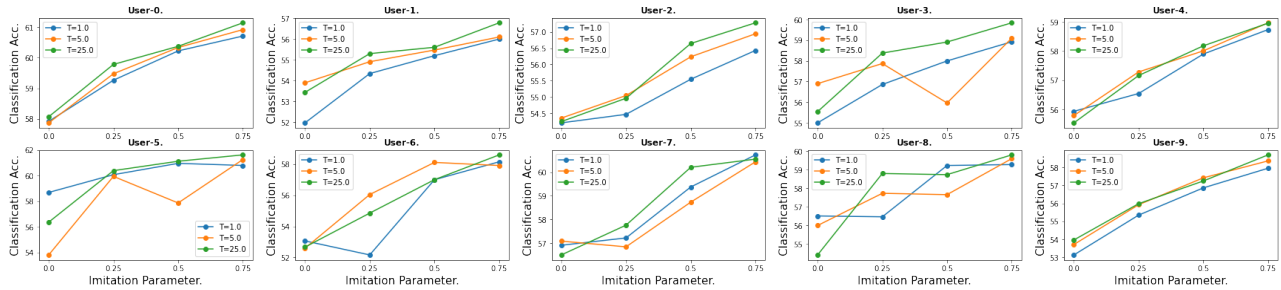


Figure 4: Per-user interaction plots between λ and T on DS-2 of CIFAR-10 averaged over the experimental runs.

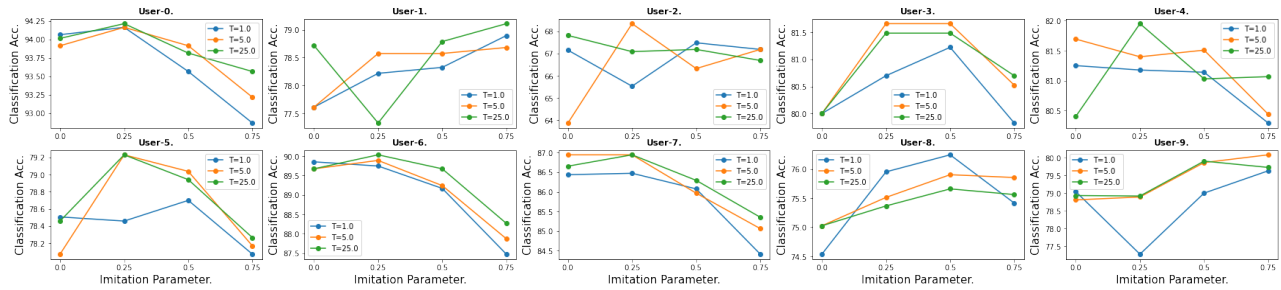


Figure 5: Per-user interaction plots between λ and T on DS-3 of CIFAR-10 averaged over the experimental runs.

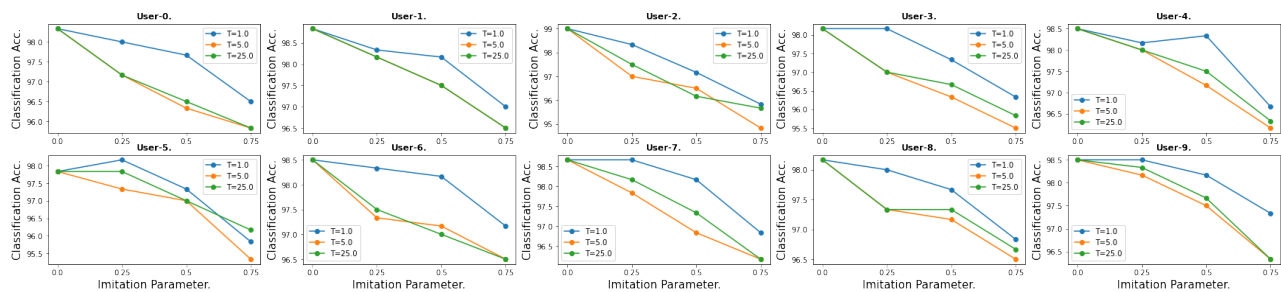


Figure 6: Per-user interaction plots between λ and τ on DS-1 of MNIST averaged over the experimental runs.

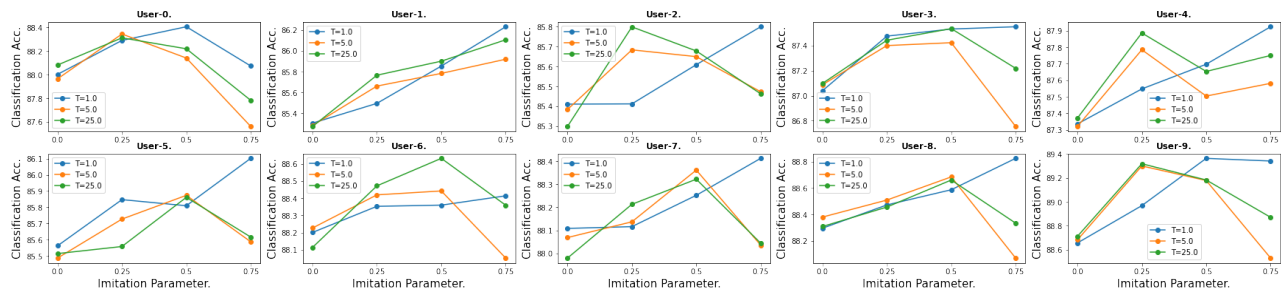


Figure 7: Per-user interaction plots between λ and τ on DS-2 of MNIST averaged over the experimental runs.

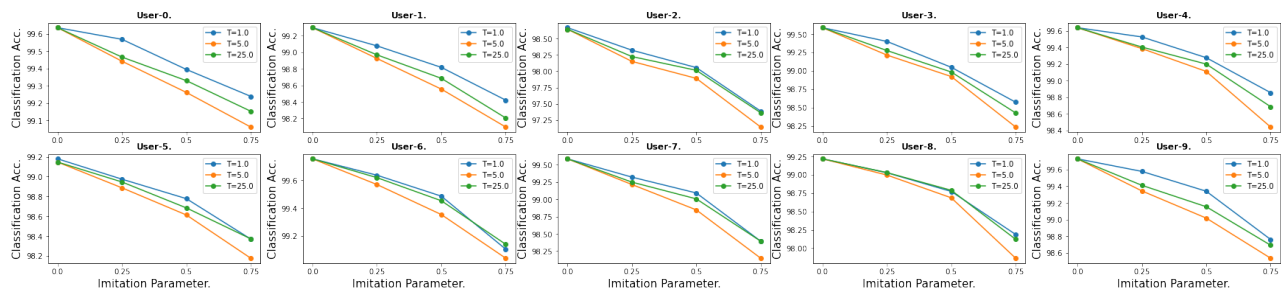


Figure 8: Per-user interaction plots between λ and τ on DS-3 of MNIST averaged over the experimental runs.